Magnetic resonance force microscopy for condensed matter
Wagenaar, J.J.T.

Cover Page

Universiteit Leiden

The handle http://hdl.handle.net/1887/50492 holds various files of this Leiden University dissertation

Author: Wagenaar, Jelmer J.T.
Title: Magnetic resonance force microscopy for condensed matter
Issue Date: 2017-07-05

6

Mechanical generation of radio-frequency fields in nuclear magnetic resonance force microscopy

WE PRESENT A METHOD for magnetic-resonance force microscopy (MRFM) with ultralow dissipation, by using the higher modes of the mechanical detector as a radio-frequency (rf) source. This method allows MRFM on samples without the need to be close to a conventional electrically driven rf source. Furthermore, since conventional electrically driven rf sources require currents that give dissipation, our method enables nuclear-magnetic-resonance experiments at ultralow temperatures. Removing the need for an on-chip rf source is an important step towards an MRFM which can be widely used in condensed matter physics.

6.1 Introduction

Magnetic resonance force microscopy (MRFM) is a technique that enables nuclear magnetic resonance experiments on the nanoscale[1]. MRFM demonstrates three-dimensional imaging with $(5 \text{ nm})^3$ resolution of a tobacco virus[2]. The technique is also exploited differently, namely in measuring spin-lattice relaxation times[3]. In both kinds of measurements, there is the need of an rf source in order to manipulate the spins. This limits the experiment in two ways: the first is the heating that occurs when large rf pulses are required[4]. The second limitation is the need for the rf source to be close to the sample under study, which increases the complexity of the experimental setup and sample preparation. In this chapter, we present a method for mechanical generation of rf fields[5], using the force sensor itself to generate the rf fields required for measuring the nuclear spin-lattice relaxation time in a copper sample, down to temperatures of 42 mK. This achievement brings MRFM one step closer to being a technique that can be more widely used in condensed matter physics or for three-dimensional imaging in biological systems at temperatures well below 1 K.

MRFM makes use of a force sensor, also referred to as the cantilever, that couples magnetically to electronic or nuclear spins due to a large field gradient. Using magnetic resonance, the spins are manipulated, such that forces or frequency shifts can be measured by the force sensor. The sensitivity of this technique for the purpose of imaging a magnetic moment μ_{min} is limited by the force noise on the sensor, and the force generated by the field gradients: $\mu_{min} = \frac{1}{\nabla B} \sqrt{4k_B T \Gamma f_{BW}}$. Here, Γ is the friction of the cantilever, currently limited by noncontact friction caused by dielectric[6] and magnetic dissipation[7]. The field gradient ∇B is generated by a micrometer-sized magnetic particle, which is typically 10^5-10^6 T/m and can be further increased using an even smaller magnetic particle[8]. The bandwidth of the measurements is given by f_{BW}. T is the temperature of the cantilever, which can be cooled and detected down to 25 mK using the superconducting-quantum-interference-device (SQUID) based readout[9]. The

[1] Poggio and Degen 2010

[2] Degen et al. 2009

[3] Isaac et al. 2016; Alexson et al. 2012

[4] Poggio et al. 2007

[5] A. M. J. den Haan, J. J. T. Wagenaar, and T. H. Oosterkamp, A Magnetic Resonance Force Detection Apparatus and Associated Methods, United Kingdom Patent No. GB 1603539.6 (1 Mar 2016), patent pending

[6] Kuehn et al. 2006
[7] den Haan et al. 2015

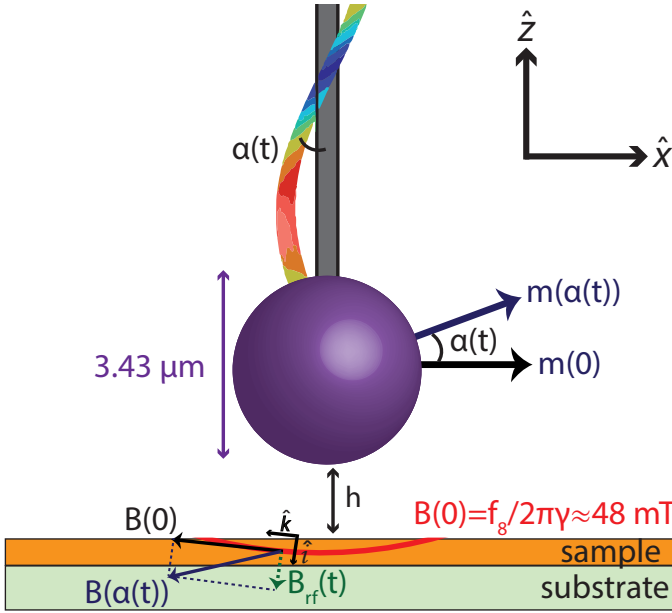[8] Overweg et al. 2015

[9] Usenko et al. 2011

Figure 6.1: Sketch of a method to mechanically generate rf fields using the higher resonant modes of the cantilever. A higher mode (rainbow beam) of the cantilever causes a rotation of the magnetic particle with an angle $\alpha(t)$. This rotation effectively results in a magnetic field component $B_{rf,a}(t)$ perpendicular to the initial magnetic field $B(0)$. Only spins that are positioned within the resonant slice, for which $B(0) = f_n/2\pi\gamma$, will be perturbed by this rf field. For the 8th mode, $B(0)$ corresponds to 48 mT and a height $h = 1.54\ \mu m$.

experiments performed on the tobacco virus are performed down to a temperature of the dilution refrigerator of 300 mK limited by the dissipation in the rf copper microwire, but with higher temperatures of the cantilever and sample caused by laser heating[10].

Our experimental setup and sample have been used recently to show that the nuclear spin-lattice relaxation time (T_1) of a copper sample can be probed at a nanoscopic scale[11] at spin temperatures as low as 42 mK. We used a superconducting rf wire to saturate ^{63}Cu and ^{65}Cu spins, causing a detectable frequency shift on the magnetic cantilever. In this experiment we found for certain rf frequencies that the number of saturated spins increased, suggesting the presence of an additional rf field. In this chapter, we show experimentally that the higher rf fields are generated mechanically by exciting higher modes of the magnetically tipped cantilever. Moreover, we report that for millisecond pulse lengths, the higher modes give rf fields much larger than can currently be obtained using the rf wire solely. When combined with an rf wire, this technique reduces the dissipation of the conventional

[10] Poggio et al. 2007; Degen et al. 2009

[11] Wagenaar et al. 2016

rf source, since less rf current is now required to obtain strong enough rf fields for MRFM experiments. When using smaller magnets, we believe that the generated rf fields can be at least 50 times larger than what is shown here, up to a few milliteslas.

6.2   *The idea*

In the case of magnet-on-cantilever geometry where the magnetic particle is attached to the cantilever, the sample experiences large magnetic field gradients and a constant magnetic field B_0. Conventionally, it is the magnetic field gradient that results in a shift of the cantilever's (first mode) stiffness[12] Δk_1, which results in a shift in the resonance frequency $\Delta f_1 = \frac{1}{2} \frac{f_1 \Delta k_1}{k_1}$. Typically, the first mode of the resonator is excited, because the sensitivity in stiffness shift is proportional to the softness of the cantilever. For the first mode, $k_1 = 7.0 \times 10^{-5}$ N/m. However, there are other available resonant modes. In magnetic force microscopy for example, torsional modes are used to improve the resolution and reduce the topography-related interference[13]. Also it has been proposed that torsional modes can be used to directly couple to a single nuclear spin inside a ferromagnet attached to a cantilever[14]. In oscillating micro- and nanoelectromechanical systems the use of multiple resonance modes of a single system can enhance the sensitivity of such systems[15]. We will show how higher modes can be used in MRFM as well, in order to mechanically generate rf fields. We propose that while the first mode, in our case at 3 kHz, is used for detection, one can use the higher modes to drive and generate an oscillating field. In Figs. 6.1 and 6.2a we sketch the idea of how the motion of higher modes results in a very small rotating magnetic field at the position of the spin, which can be decomposed in a static field and an oscillating rf field.

The idea is as follows. The magnetic particle with magnetic moment m gives a magnetic field $B(r, t)$ at the spin's location r. For a spherical particle this is a dipole mag-

[12] De Voogd et al. 2017

[13] Kaidatzis and García-Martín 2013

[14] Butler et al. 2010

[15] Reiche et al. 2015

netic field:

$$B(r,t) = \frac{\mu_0}{4\pi} \left(\frac{3r(m(t) \cdot r)}{r^5} - \frac{m(t)}{r^3} \right) \qquad (6.1)$$

When the force sensor is at rest, the magnetic moment of the cantilever is oriented in the x direction, along the direction of motion of the fundamental mode. But when a higher mode with frequency f_n is driven, the particle starts to rotate with an angle $\alpha(t) = \alpha_0 \sin(2\pi f_n t)$, see Fig. 6.1. Assuming that the magnetic particle rotates at a frequency f_n, we can write the magnetization and the magnetic field as follows:

$$
\begin{aligned}
m(t) &= m \cos(\alpha(t))\hat{x} + m \sin(\alpha(t))\hat{z} \\
&\approx m\hat{x} + \alpha_0 m \sin(2\pi f_n t)\hat{z}
\end{aligned}
\qquad (6.2)
$$

Here, we assume in the last line a small rotation angle. The magnetic field $B(r, \alpha(t))$ will only deviate a bit from the rest position, and thereby the orientation of the spin will be almost constant. However, we know from conventional NMR that a very small perpendicular rf field with the right frequency can cause large perturbations in the spin's alignment when the field oscillation is resonant with the Larmor frequency[16]. The perpendicular component of the magnetic field with respect to the magnetic field at $t = 0$ can be seen as such a perpendicular perturbing rf field $B_{rf,a}(r, \alpha(t))$:

[16] Abragam 1961

$$|B_{rf,a}(r, \alpha(t))| = \frac{|B(r, \alpha(t)) \times B(r, 0)|}{|B(r, 0)|} \qquad (6.3)$$

$B_{rf,a} \propto \alpha$ for small α. Neglecting the small parallel component, we can write the magnetic field $B(r, t)$ as

$$B(r,t) = |B(r, 0)|\hat{k} + |B_{rf,a}(r, \alpha_0)| \sin(2\pi f_n t)\hat{i} \qquad (6.4)$$

In the local coordinate frame of the spin, with $\hat{k}$ parallel to $B(r, 0)$ and $\hat{i}$ chosen parallel to $B_{rf,a}(r, \alpha(t))$. This is again conventional NMR with an alternating rf field $B_{rf,a} \equiv |B_{rf,a}(r, \alpha_0)|$, giving resonance when the frequency of the rotation f_n is equal to the Larmor frequency of the spins $f_L = \frac{\gamma}{2\pi} B_0$.

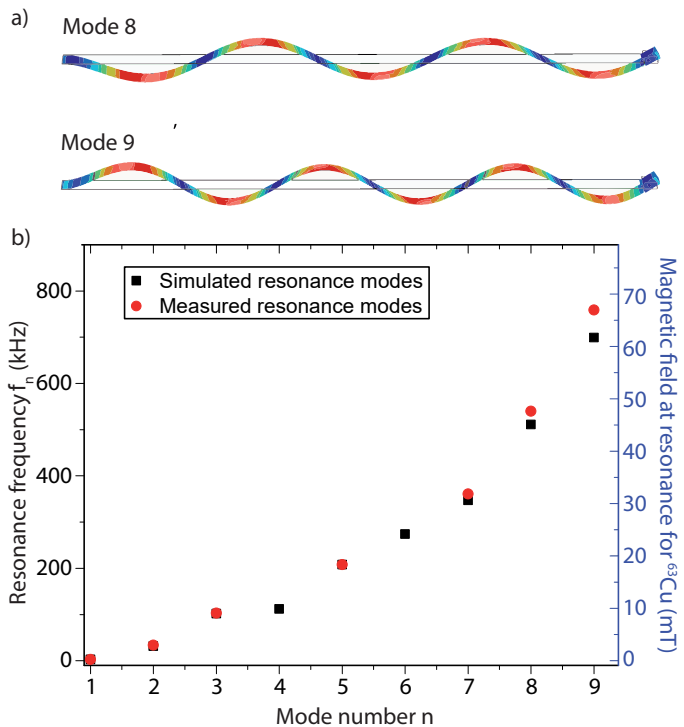In an MRFM experiment, the cantilever is also driven at its fundamental mode. Since this frequency is very low

compared to the Larmor frequency of the spins, the motion at the fundamental mode will be well off resonance. However, one can expect a broadening of the slice, since it will move along with the static magnetic field. This effect can be diminished by the use of active feedback cooling on the fundamental mode[17].

In our case, we work with a magnet attached to the cantilever, but we believe the idea holds also for an MRFM with sample-on-tip geometry[18].

[17] Vinante et al. 2012

[18] Degen et al. 2009

Figure 6.2: **a)** Simulation of the 8th and 9th mode of the cantilever. These two modes are used in the experimental part of this chapter. The dynamics of the magnetic particle at higher modes are mainly rotational, which is due to the relatively larger mass of the magnetic particle compared to the bare silicon cantilever. **b)** Frequency of the simulated (black) and measured (red) modes of the cantilever. Modes 4 and 6 do not oscillate in the x direction and could therefore not be detected. On the right vertical axis the corresponding magnetic field at resonance ($f_n = \frac{\gamma}{2\pi} B_0$) for the ^{63}Cu is shown.

6.3 Experiment

6.3.1 Setup

The setup consists of the force detector and a copper sample sputtered on top of a detection chip. A detailed description of the setup can be found in Refs. (Wagenaar et al., 2016; Den Haan et al., 2015). Here, we will only

give a short summary. The force sensor is a very soft
IBM-type silicon cantilever, with $k_1 = 7.0 \times 10^{-5}$ N/m,
and length, width and thickness of 145 μm, 5 μm and 100
nm respectively[19]. Using electron-beam-induced deposi-
tion, a spherical NdFeB magnetic particle with a radius of
1.72 μm and a saturation magnetization of 1.15 T is glued
to the end of the cantilever, resulting in a fundamental
resonance frequency of $f_1 = 3.0$ kHz, and a mechanical
quality factor of $Q_1 = \frac{k_1}{2\pi f_1 \Gamma} = 2.8 \times 10^4$ at cryogenic tem-
peratures. The cantilever can be moved on a range of
1 mm using an in-house-developed cryopositioning sys-
tem, while measuring the absolute position using capac-
itive sensors. A fine stage below the sample can be used
to scan the sample in a range of 2.3 μm. The cantilever is
driven using a piezoelectric element[20].

The detection chip consists of a superconducting pickup
loop, 30×30 μm^2, connected to a superconducting quan-
tum interference device (SQUID). The motion of the mag-
netic particle results in a flux change in the pickup coil,
measured by the SQUID[21]. Close to the pickup coil, cop-
per is sputtered on an area of 30×30 μm^2 with a thickness
of 300 nm and a roughness of 10 nm. A gold capping layer
is sputtered in order to prevent oxidation of the copper.
The copper sample is thermalized to the mixing chamber
of the dilution refrigerator using a patterned copper wire
leading to a large copper area, which is connected to the
sample holder via gold wire bonds. The sample holder is
connected via a welded silver wire to the mixing cham-
ber. A superconducting (Nb,Ti)N rf wire, 2 μm wide and
300 nm thick, is positioned from the copper sample at a
distance of 500 nm. For the experiments in this chapter,
we position the cantilever above the copper, close to the rf
line (7 ± 1 μm) and close to the pickup coil (5 ± 1 μm).

[19] Chui et al. 2003; Mamin et al. 2003

[20] Piezoceramic Tube 5A by EBL
Products, Inc., USA; PICMA Chip
Monolithic Multylayer Piezo Actua-
tor PL033.30 by Physik Instrumente
(PI) GmbH & Co., Germany.

[21] Usenko et al. 2011

6.3.2 Higher modes

Besides the cantilever's fundamental resonant mode in
the x direction, at $f_1 = 3.0$ kHz, the cantilever exhibits
many higher modes. We simulated the eigenmodes using
a finite element analysis (COMSOL MULTIPHYSICS) with
an eigenfrequency study. The results of the mode shapes

for the 8th and the 9th mode are visible in Fig. 6.2a. Some modes, 4 and 6, are motions that do not oscillate in the x direction, which give too small flux change in the pickup coil to be detected. We are able to detect the higher modes by driving the cantilever using the rf wire, as well as by using the piezoelectric element located on the holder of the cantilever. Figure 6.2b shows a graph of the simulated and the measured resonance frequencies of the cantilever.

Most of the higher modes are similar to the 8th and 9th modes, but with less or more nodes. The node present at the position of the magnetic particle results in a rotation of the magnetic moment m. In this chapter, we will use only modes 8 and 9. The even higher modes have resonant slices corresponding to a shorter distance. The eddy currents in the copper prevented us from measurements closer than approximately 1 μm distance. The lower modes have the disadvantage that the corresponding signals would be much less, since the required distance would be larger. We believe that the method described in this chapter can also be applied to other modes with a rotation of the magnetic particle, up to the megahertz regime. These modes would be available when studying a less dissipative sample.

6.3.3   Measurement protocol

In this experiment, we initially follow the same measurement protocol as used when the rf wire is used as a conventional electrically driven rf source. However, by applying shorter pulses with the rf wire, and by applying pulses with a piezoelectric element attached to the cantilever holder, we show that we can excite the higher modes of the cantilever, resulting in a larger magnetic field strength as is obtained by using only the rf wire.

When an rf field $B_{rf,a}$ is applied perpendicular to the direction of the magnetic field which is parallel to the spin's initial orientation, the spin will rotate around the axis of rotation[22] parallel to $B_{rf,a}$. For large rf fields and sufficiently long pulses, the spin transitions saturate, resulting in a net-zero magnetization for ensembles of spins. The average contribution of a single spin in this ensemble

[22] Abragam 1961

causes a stiffness shift and, therefore, a frequency shift $-\Delta f_s$. Only the spins that meet the resonance condition $f_{rf} = \frac{\gamma}{2\pi} B_0$, with γ the gyromagnetic ratio, will be excited, thus forming the resonant slice. The total frequency shift $-\Delta f_1$ can be obtained by summation of all spins within the resonant slice,

$$\Delta f_1 = -p \sum_V \Delta f_s(\boldsymbol{r}) \qquad (6.5)$$

Here, p is the net Boltzmann polarization of the nuclear spins.

We drive the cantilever at its resonance frequency f_1 using a phase-locked loop (PLL) of a Zurich Instrument lock-in amplifier to measure the frequency shifts. During the pulse, the PLL is switched off, driving the cantilever at its last known resonance frequency, to avoid possible cross-talk effects. The small frequency shifts and the cantilever's low Q factor enable the PLL to drive well within the cantilever's linewidth during the pulse, thereby keeping the oscillation amplitude of the cantilever constant.

After a saturation pulse, the nuclear spins will exponentially restore their initial orientation in a characteristic time T_1. For copper, the relaxation time follows the Korringa relation[23] $TT_1 = 1.2$ sK, which is confirmed in the experiments with the rf wire as the rf source[24]. After a saturation pulse ending at $t = 0$, the frequency shift evolves as function of time $\Delta f(t)$ according to:

$$\Delta f(t) = -\Delta f_1 e^{-t/T_1} \qquad (6.6)$$

[23] Korringa 1950

[24] Wagenaar et al. 2016

6.3.4   Results

Figure 6.3a shows the frequency shift Δf_1, according to Eq. 6.6, after applying a 1-s pulse with the rf wire[25], at a temperature of 42 mK. We use a current of $I = 0.2$ mA, resulting in an alternating rf field of $B_{rf,a} = (\mu_0 I / 2\pi r) \approx$ 5.8 μT. The magnetic field strength is enough for a saturation parameter which is at least $s \equiv \gamma^2 (B_{rf,a}/2)^2 T_1 T_2 \approx$ 30, which indicate that for sufficiently long pulse times the spins will saturate at least 95%. However, the rf field generated leads to a flipping rate of approximately $\gamma B_{rf,a}/4\pi \approx$

[25] Wagenaar et al. 2016

Figure 6.3: **a)** Frequency shift of the cantilever's first mode at 3 kHz after applying an rf pulse of 0.2 mA and a 1-s length using the rf wire. In blue, the data (Wagenaar et al., 2016) was measured at a height of 1.54 μm and a temperature of 42 mK. The solid line is numerically calculated (Eq. 6.5) using a resonant slice thickness of 38 nm. In red is the simulated signal when the cantilever is positioned 400 nm closer to the surface. The dotted lines indicate the positions of the higher modes $f_8 = 542 \pm 1$ kHz and $f_9 = 759 \pm 1$ kHz. **b)** Frequency shift as a function of time after applying an rf pulse at the frequency of the two higher modes at $T = 77$ mK. The pulse time of 11 ms is too short to saturate the spins directly with the oscillating magnetic field of the rf line, but the excitation of the higher modes gives a large-enough rf field. As expected from (a), no signal is observed at the mode of 759 kHz, while there is for the mode at 542 kHz. **c)** The same as in (b), but the cantilever has been moved 400 nm closer to the sample. The mode at 759 kHz now corresponds to a resonant slice that lies within the sample, resulting in a frequency shift, while the signal at 542 kHz is greatly reduced. Note (b) and (c) are measured at slightly larger temperatures, and have much shorter pulse lengths than (a).
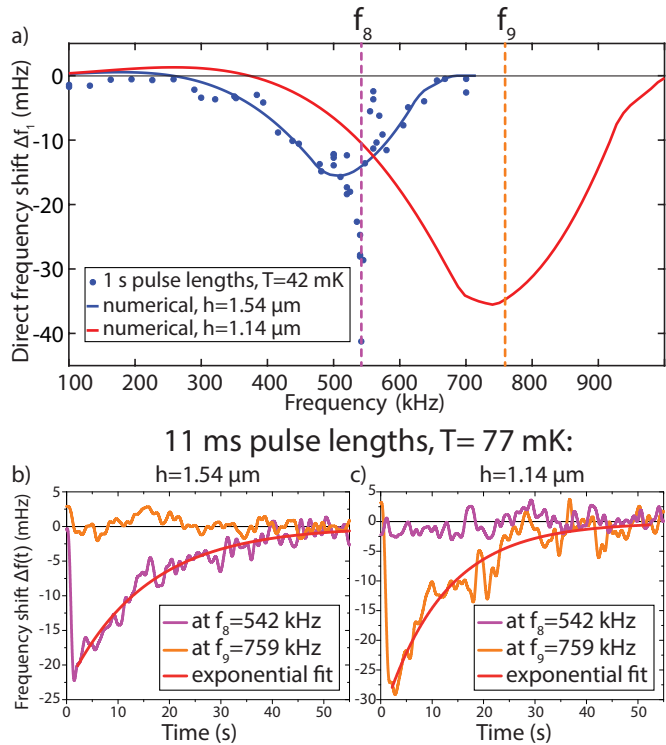
30 Hz, which is not fast enough to saturate the spin levels within milliseconds. The solid blue line in the figure is the calculated signal with a height above the sample $h = 1.54$ μm and slice thickness $d = 38$ nm. The yellow curve is the simulated signal with the same slice thickness, but at a different height, 400 nm closer to the surface. The dashed vertical lines are the indicated positions of the 8th and 9th mode of the cantilever. Visible in blue is that we obtain a much larger signal when the radio frequency applied corresponds to the 8th mode, which we attribute to a much larger $B_{rf,a}$ field, since the resonant slice thickness grows at sufficiently large rf field strengths[26].

To confirm that the larger rf fields are generated by the rotation of the magnetic particle when the higher mode is driven by the rf wire, we measure the signal for much shorter rf pulses. At a pulse length of 11 ms no frequency shifts are found, except when the frequency is equal to a higher mode and when the frequency of this mode has a resonant slice in the sample. In Figs. 6.3b and 6.3c, typical time traces are shown, after an 11-ms rf pulse with a frequency that matches exactly the 8th and 9th mode at a temperature of $T = 77$ mK. The pulse time of 11 ms is too short to saturate the spins directly with the $B_{rf,a}$ of the wire. We see that the 9th mode does not give any signal at $h = 1.54$ μm, but after approaching the cantilever to the sample by 400 nm, we obtain a clear signal, while the signal at the 8th mode vanishes. We average multiple time traces, with a low pass filter with a cutoff frequency of 1 Hz to smooth the data.

The relaxation times fitted in Figs. 6.3b and 6.3c ($T_1 \approx$ 15 s and $T_1 \approx 12$ s) with the temperature $T = 77$ mK, result in $TT_1 \approx 0.9 - 1.2$ sK, in agreement with the well-known bulk measurement[27] of $TT_1 = 1.2$ sK. In the previous report[28], this relation was measured for a wider range of temperatures, also for the data collected at the frequency at the 8th mode, showing the same relation.

Figure 6.4 shows two averaged time traces for two different methods to excite the higher mode. We use the superconducting rf wire to excite the cantilever. The cantilever can be positioned far from the rf wire, enabling ex-

[26] Wagenaar et al. 2016

[27] Pobell 2007

[28] Wagenaar et al. 2016

Figure 6.4: Exciting the cantilever with the rf line (blue) with a current of 0.2 mA and pulse length of 11 ms, and with the piezoelectric element (green) on the cantilever's mount stage with a pulse length of 4 ms.
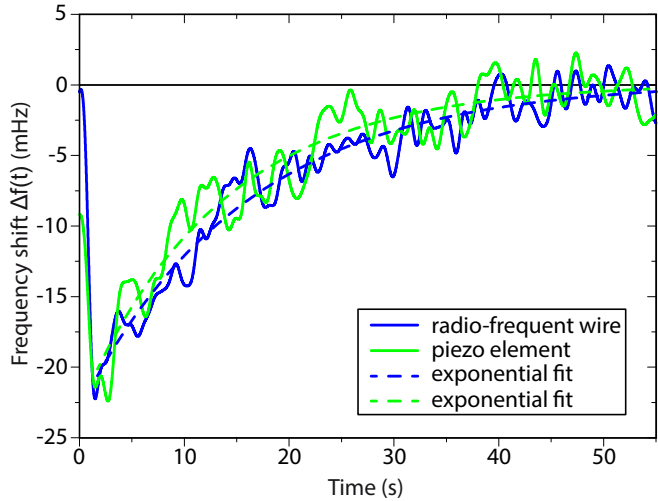
[29] Degen et al. 2009

periments on a much larger area than in previous MRFM experiments[29]. On top of this, no significant heating is present within this experiment, since very low rf currents are already sufficient for driving the cantilever (see Fig. 6.5).

Furthermore, we report on experiments in which we do not use the rf wire as a driving mechanism, but solely drive the cantilever using the piezoelectric element to excite the fundamental cantilever motion in the phase-locked loop mode. Here, we follow the same measurement procedure, but instead of applying the pulse using the wire, the signal is added to the piezoelectric element. We excite the piezoelectric element at $f_8 = 542$ kHz for a very short period of 4 ms with a voltage of 200 mV, and do not see an increase in frequency shift when applying larger voltages. Figure 6.4 shows an equal frequency shift is obtained for both methods, which could be an indication of an intrinsic limitation of the rotation angle of the higher modes.

To investigate the possible limitations of the amplitude of the rf fields generated by the higher modes, we need to investigate the maximal rotation angle α that can be obtained. Figure 6.5 shows the SQUID signal while sweeping the frequency of the current through the rf wire, with the cantilever positioned far from the surface. We see
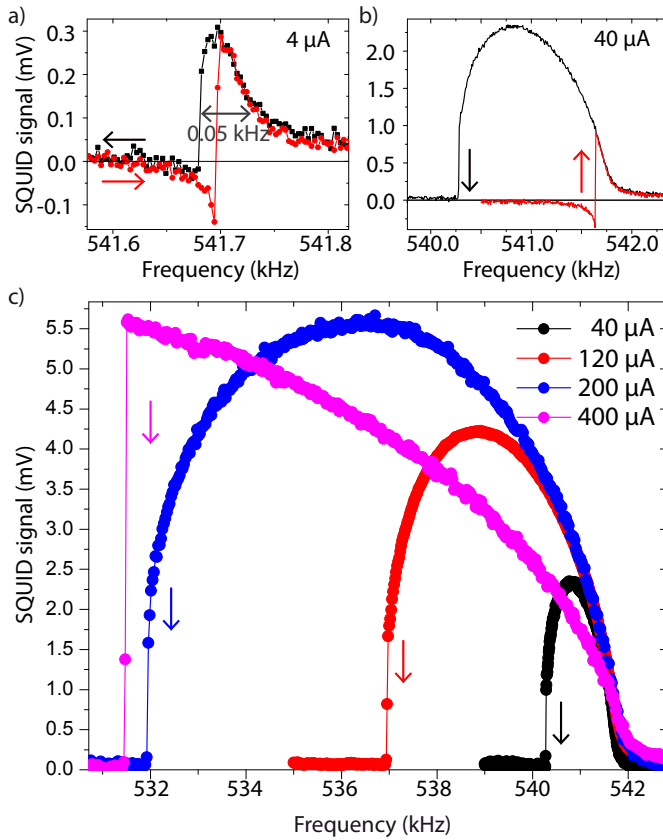
Figure 6.5: **a,b)** Exciting the cantilever at its 8th mode, far from the surface, by sweeping the frequency by using the rf wire while recording the SQUID's signal. Already at a current of 40 μA, a huge nonlinear effect (Duffing) is present. A background signal is subtracted for clarity. **c)** The sweeps from right to left at different currents.

[30] Hamel 1921

that even for small rf currents the higher modes behave nonlinearly (Duffing), visible by the hysteresis and typical foldover effect[30] when performing a frequency sweep from left to right and vice versa. For 4 μA, we have minimal hysteresis, enabling us to estimate the quality factor on the order of $Q_8 \approx 10^4$.

We can give a lower bound for the field strengths by observing the amplification we see of the signal at the frequency of the higher mode and compare it with the signal which one would have expected using only the rf wire. Figure 6.3a shows that the amplification is almost a factor of 3. The resonant slice thickness is proportional to the rf field strength in the saturation regime[31], neglecting possible spin diffusion. From this, we obtain a lower bound of approximately 18 μT. By using Eq. 6.3, we calculate that this field strength corresponds to a rotational angle of only $\alpha_0 \approx 0.01$ deg. This angle corresponds to an amplitude of the mode's antinodes of only $\delta x_8 \approx \frac{\alpha_0 L}{10} \approx 1$ nm, with L the length of the cantilever, and α_0 in radians.

[31] Wagenaar et al. 2016

6.4   Discussion and outlook

One of the difficulties of performing MRFM experiments at millikelvin temperatures is the power dissipation of the rf source. Poggio et al.[32] used a copper microwire as the rf source, with a dissipated power of 350 μW at an rf field strength of 4 mT. To compare the power dissipation of the cantilever with the copper microwire, we can quantify the thermal efficiency of the rf source in terms of the dissipated power for a given field strength in units W/T^2. The dissipated power, due to friction, when driving the cantilever at its 8$^{\text{th}}$ mode is given by $P = \Delta E f_8 = \frac{2\pi^2 m_{eff} f_8^3 \delta x_8^2}{Q_8}$. Substituting $Q_8 = 10^4$, amplitude $\delta x_8 = 1$ nm, $f_8 = 542$ kHz, and effective mass[33] $m_{eff} = 2 \times 10^{-13}$ kg, we obtain a dissipated power of $P \approx 6 \times 10^{-17}$ W. This results in a thermal efficiency of $\frac{6 \times 10^{-17} \text{W}}{(18 \mu T)^2} = 0.2$ μW/T^2, which is a thermal efficiency of 8 orders of magnitude better than obtained using the copper microwire. In this calculation we do not take into account the dissipation of the driving mechanism, in our case the superconducting rf wire

[32] Poggio et al. 2007

[33] den Haan et al. 2015

or the piezoelectric element. Since we do not observe any temperature increase, even at much larger currents and voltages, we can estimate this dissipation to be much lower than of the order nanowatts. Even if this dissipation is limiting, it will stay constant when our mechanism is used in a more optimal setup, resulting in much larger field strengths, as discussed below.

Saturation experiments do not need large rf fields, so the rf fields we mechanically generate are enough for measurements of the nuclear spin-lattice relaxation times in condensed matter systems. However, if one would like to use this technique for high-resolution three-dimensional imaging, one would need much larger rf fields. The reason for this is that, in order to exploit the MRFM fully, one would like to flip the spin exactly twice every period for the fundamental cantilever mode. For example for protons, magnetic field strengths of several milliteslas are needed to use this protocol[34]. We obtain at least 18 μT, probably hampered by the huge hysteresis of the higher mode. However, this field is achieved at a large separation between the cantilever and the surface to reduce the impact of the eddy currents which affect the quality factor of the fundamental mode at 3 kHz. When we perform the experiment directly above the sample, we gain a factor of 6 in the rf field strength. When using smaller magnetic particles of focused ion-beam milled FePt[35], we gain an additional factor of 8. This can be further improved by using magnets with even larger field gradients[36]. We believe that these improvements would bring the intensity of the rf field up to the mT range, which would allow the adiabatic rapid passages needed for high-resolution three-dimension MRFM imaging[37].

The resolution of this experiment can be expressed in two ways. For a simplified data analysis, the measurement shown in Fig. 6.3a gives information in one dimension for a sample which is homogeneous in the other dimensions. In this case, the thickness of the resonant slice is a measure for the resolution. We find for the measurements of Figs. 6.3 and 6.4 a slice thickness of approximately 50 nm.

[34] Poggio et al. 2007

[35] Overweg et al. 2015

[36] Tao et al. 2016

[37] Poggio et al. 2007

[38] Degen et al. 2009

[39] Wagenaar et al. 2016

When the measurement is repeated many times at different cantilever positions, the slice thickness is not going to be the limiting factor for the resolution. Careful deconvolution of the obtained signal with the point-spread function of the magnetic particle can result in a much higher resolution[38]. Therefore, a better measure of resolution is the signal-to-noise ratio of the measurement given a certain bandwidth. For this, we can use the results of the previous report[39], where the conventional electrically driven rf source is used, to obtain a volume sensitivity of $(30 \text{ nm})^3$, within a bandwidth of 1 Hz.

6.5   Conclusions

To summarize, we demonstrate a mechanical method to generate rf fields using the higher modes of a cantilever. This method can be used within MRFM experiments while using the same cantilever also as force sensor by measuring the frequency shift of the much softer first resonant mode. Our method enables MRFM without being limited by being too close to a conventional electrically driven rf source. Furthermore, it prevents the usual heating of sample and cryostat at millikelvin temperatures. We have shown that the field strength can be extended to the millitesla regime by using higher field gradient magnets, allowing this technique to be used in the more advanced imaging methods in MRFM. All together, we believe that this method constitutes a major contribution towards the development of MRFM at ultralow temperatures.

Acknowledgements